ARTICLE TYPE

Structural disorder in molecular framework materials†

Andrew B. Cairns and Andrew L. Goodwin*

Received Xth XXXXXXXXXX 20XX, Accepted Xth XXXXXXXXX 20XX
First published on the web Xth XXXXXXXXXX 200X
DOI: 10.1039/b000000x

It is increasingly apparent that many important classes of molecular framework material exhibit a variety of interesting and useful types of structural disorder. This tutorial review summarises a number of recent efforts to understand better both the complex microscopic nature of this disorder and also how it might be implicated in useful functionalities of these materials. We draw on a number of topical examples including topologically-disordered zeolitic imidazolate frameworks (ZIFs), porous aromatic frameworks (PAFs), the phenomena of temperature-, pressure- and desorption-induced amorphisation, partial interpenetration, ferroelectric transition-metal formates, negative thermal expansion in cyanide frameworks, and the mechanics and processing of layered frameworks. We outline the various uses of pair distribution function (PDF) analysis, dielectric spectroscopy, peak-shape analysis of powder diffraction data and single-crystal diffuse scattering measurements as means of characterising disorder in these systems, and we suggest a number of opportunities for future research in the field.

1 Introduction

Throughout many of the highest-profile areas of research within contemporary solid state science—from spin frustration in cooperative paramagnets[1] to thermoelectrics[2] through to polar nano-domain formation in relaxor ferroelectrics[3]—*dis*order plays a central role in driving function. Yet in the field of molecular framework chemistry much of the research emphasis remains on developing and characterising highly-crystalline and well-ordered systems.[4] In this tutorial review, we explore some of the few—but important—emerging families of well-characterised disordered molecular frameworks. Our emphasis is on highlighting how structural disorder can also give rise to interesting and unusual physical properties in this long-established class of materials.

There are good reasons why molecular frameworks (including the ubiquitous metal–organic frameworks, or MOFs) might be expected to exhibit interesting forms of structural disorder. First, the very nature of their underlying design principle—the linking of nodes (usually transition metals or metal clusters) by extended molecular bridges [Fig. 1(a)]—is inherently predisposed to the formation of flexible materials with open structures.[5] Since many molecular frameworks are porous, then large amplitude displacements of the framework linkers can dominate the dynamical behaviour if these pores are empty; likewise dynamic reorientation of guest molecules can dominate if the pores are filled. A second point is that the energetics of molecular frameworks are dominated not by long-range electrostatic forces (which play an important role in stabilising *e.g.* oxide-based framework structures) but by covalent bonds within the molecular linkers, on the one hand, and localised polar/covalent interactions between the metal centres and ligand donor atoms on the other hand. Consequently, minimisation of the lattice enthalpy often requires only that local bonding geometries be optimised, and so there may be very little enthalpic difference between crystalline and amorphous forms—so long as the local bonding arrangements are similar in both. In the study of conventional glass-forming materials, it is well established that network topology and connectivity also play a crucial role in stabilising disordered states[6]—and these are precisely the parameters over which the materials chemist has extraordinary control in the synthesis and design of molecular frameworks. So there is a sense not only that these systems might be somewhat predisposed to disorder, but also that this disorder might readily be tuned through exploitation of the versatile structural chemistry of this broad family [Fig. 1(b,c)].

The term "disorder" can be unhelpful because it is taken to encompass a very large number of different phenomena.[6] Here we focus primarily on four specific aspects—topological, static, dynamic, and low-dimensional disorder [Fig. 1(d)]—chosen for their relevance to the key studies in the field. We explain what we mean by each of these in turn, with the four topics assuming a thematic role for each the four main sections of the review. Where appropriate, we include discussion of relevant experimental techniques, computational approaches, and theoretical models used to characterise and interpret these various types of disorder. We conclude with a brief discussion of some interesting examples of disorder that do not obviously fit into the four principal categories, which we place in the context of a distinctly personal perspective on

Department of Chemistry, University of Oxford, Inorganic Chemistry Laboratory, South Parks Road, Oxford OX1 3QR, U.K. Fax: +44 (0)1865 272690; Tel: +44 (0)1865 272137; E-mail: andrew.goodwin@chem.ox.ac.uk

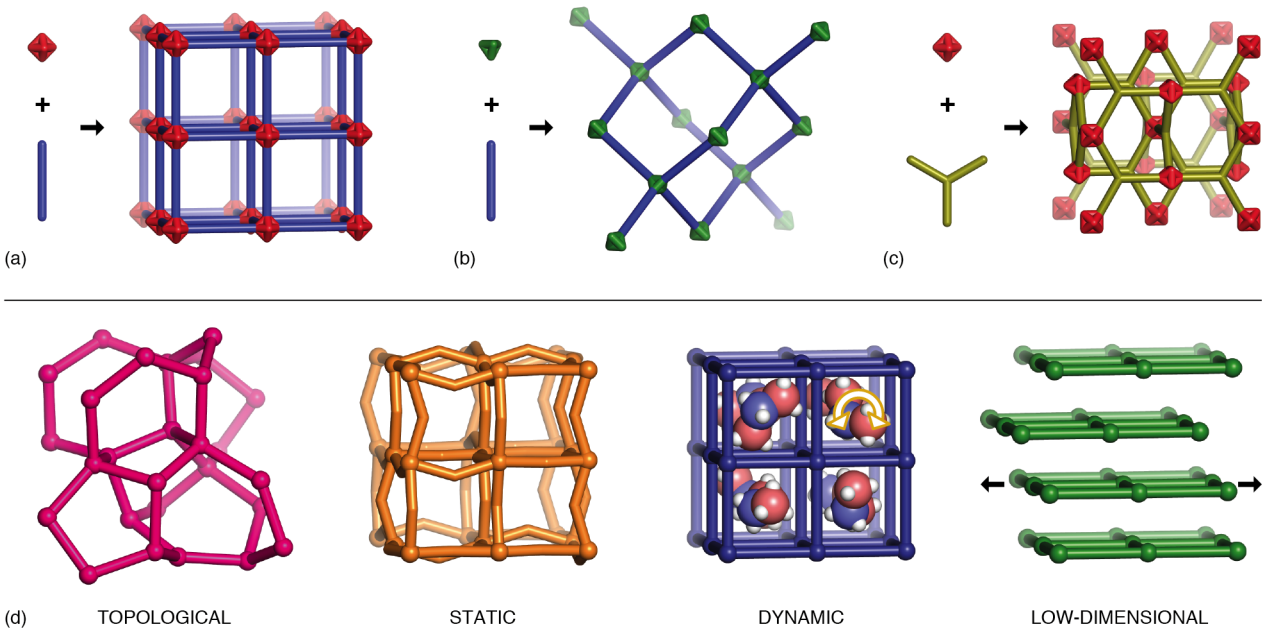

Fig. 1 Order and disorder in molecular frameworks. (a) The basic design strategy for molecular frameworks involves the linking of nodes (here, red octahedra) by molecular bridging units (here, blue rods) to form a three-dimensional open network. By using (b) nodes and/or (c) linkers of different connectivities it is possible to access a very large number of different network topologies.[7] (d) Some of the possible mechanisms by which structural disorder can be introduced into molecular frameworks include: (left–right) topological disorder, where the network itself is inherently aperiodic; static disorder, where regions of the framework under large distortive displacements that are not strongly correlated from one region of the structure to another; dynamic disorder, where some component of the framework (often a guest or counterion occupying the pore system) thermally samples multiple different configurations; and low-dimensional disorder, where the absence of strong bonding interactions in one more directions results in a lack of registration between neighbouring layers or columns of the framework.

how the field might develop over the coming years.

2 Topological disorder

The existence of framework topologies with well-defined local geometries but with no long-range periodicity has been recognised for many decades. Perhaps the canonical example is that of silica glass (*a*-SiO_2). The existence of an amorphous state of silica is attributed to the accessibility of a "continuous random network" (CRN) phase,[8] in which all of the Si and O atoms adopt nearly-ideal bonding geometries—hence the lattice enthalpy is comparable to that of the crystalline SiO_2 polymorphs—and yet the network itself does not exhibit any long-range structural periodicity [Fig. 2(a)].[9] Indeed the CRN model is the basis of much of our understanding of glassy systems, including the amorphous allotropic forms of group 14 elements such as silicon and germanium. Entropy is thought to play a key role in stabilising these networks, for the simple reason that there are many more CRN-type configurations than there are ordered networks of comparable lattice enthalpies. Because there is no pathway for converting a CRN phase such as *a*-SiO_2 into any crystalline polymorph without making and breaking bonds, and because CRNs are aperiodic (they have no unit cell), such systems can be said to be *topologically* disordered.

From an experimental viewpoint, the absence of long-range structural periodicity in topologically-disordered systems has a number of observable consequences.

1. Their X-ray, neutron and/or electron diffraction patterns do not contain any Bragg reflections but consist instead of a smoothly-varying diffuse scattering contribution that has no orientational dependence. The Fourier transform of this scattering pattern gives a pair distribution function (PDF) that reflects at once both the strong local order and vanishing long-range order implied by the CRN model.

2. The absence of translational periodicity removes vibrational selection rules; consequently all vibrational modes of a topologically-disordered solid are both Raman and infrared active.

3. Such materials are inherently isotropic—*i.e.* their physical properties have no orientational dependence. This includes mechanical properties (bulk and shear moduli,

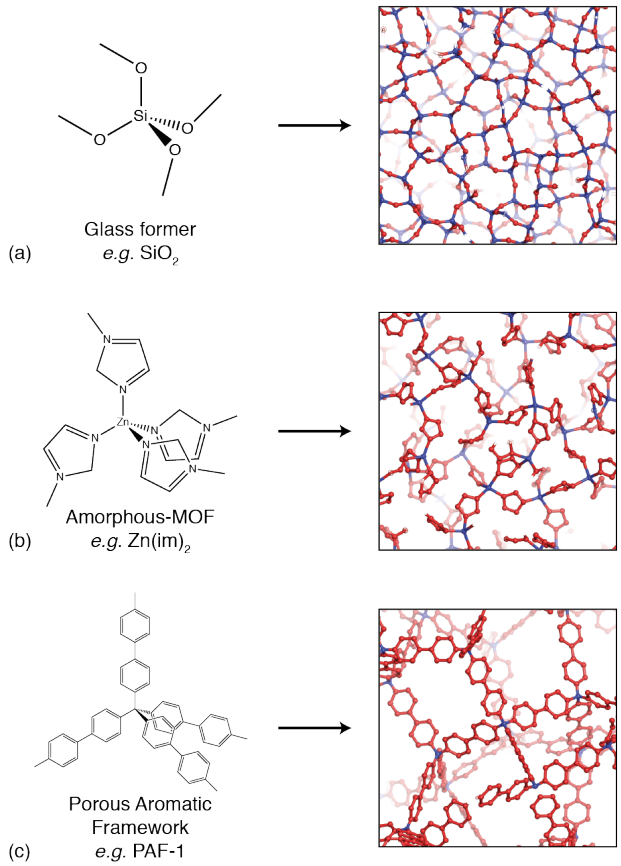

Fig. 2 CRN descriptions of some framework materials. (a) The CRN phase of silica consists of tetrahedrally-coordinated Si atoms connected via O atoms with approximately-ideal O–Si–O and Si–O–Si angles. The various bond length, bond-angle and torsion-angle distributions in this phase are remarkably similar to those in the crystalline polymorph α-cristobalite, despite the absence of any long-range structural periodicity (the network shown here has no unit cell).[9] (b) Substitution of the Si and O atoms in this CRN by Zn and imidazolate species, followed by suitable expansion of the network to give reasonable bond lengths, yields a CRN of composition Zn(*im*)$_2$ that can be refined successfully against neutron and X-ray PDF data.[10] (c) The same CRN can be used to build a candidate model for the structure of PAF-1.[11] The accessible surface area calculated using this model agrees well with the experimental density and with N_2 sorption measurements.

thermal expansivities) and optical properties (absorption, refraction) alike.

It is likely that topologically-disordered molecular frameworks have been synthesised by many groups for many years, but it is only relatively recently that well-characterised examples have appeared in the literature. This disconnect is almost certainly due to the experimental difficulty of characterising amorphous frameworks: their chemical composition, phase purity, and density are often difficult to determine; moreover, it is only relatively recently that robust X-ray PDF methods have become accessible to the materials chemist.[12] We focus here on the particular case of zeolitic imidazolate frameworks (ZIFs)—a family of molecular frameworks which have been well-studied both for their high thermal and chemical stabilities and for their promising applications as gas-storage candidates.[13] The structural chemistry of ZIFs is straightforward: tetrahedrally-coordinated dications (usually Zn^{2+} or Co^{2+}) are linked *via* imidazolate (im^-) or substituted imidazolate linkers. The Zn–*im*–Zn angle is similar to the Si–O–Si angle in silica polymorphs, and so ZIFs can adopt many of the network topologies found in (alumino)silicates—including porous zeolite-like structures.

On heating to temperatures of *ca* 300 °C, a number of porous crystalline ZIF polymorphs undergo a framework collapse that results in the adoption of a common dense topologically-disordered phase with the same Zn(*im*)$_2$ composition as the crystalline precursors.[10,14] This temperature-induced amorphisation (TIA) process can be monitored using optical microscopy (the originally anisotropic crystallites become isotropic) and/or using diffraction methods (the Bragg peaks vanish and are replaced by a smoothly-varying diffuse scattering pattern) [Fig. 3]. The amorphous "*a*-ZIF" phase so formed is metastable and can be recovered to ambient conditions. Mechanical measurements performed on recovered samples also reflect the loss of mechanical anisotropy expected for a topologically-disordered material. Subsequent heating to *ca* 400 °C gives rise to a second transformation: this time from the amorphous ZIF phase to the densest of the known crystalline ZIF polymorphs, ZIF-zni.[10] The identical composition of initial and final crystalline compounds unambiguously identifies the composition of the disordered intermediate.

There is strong experimental evidence from neutron and X-ray PDF measurements to support an interpretation of the structure of *a*-ZIFs in terms of the same CRN model applied to model systems such as *a*-SiO_2 [Fig. 2(b)].[10] High-resolution neutron PDFs indicate that the local coordination environment in *a*-ZIFs is essentially identical to that found in the corresponding crystalline ZIF polymorphs [Fig. 3]. Moreover, the variation in PDF peak intensity with increasing distance shows remarkable qualitative similarity to that observed in *a*-SiO_2 (taking into account the necessary change in length scale associated with the replacement of Si–O–Si linkers by Zn–*im*–Zn linkers). But perhaps most crucially, a model of the structure of *a*-ZIF derived from the SiO_2 CRN can actually be refined quantitatively against the experimental neutron and X-ray PDF data. Such a fit is carried out in a similar fashion to the way in which *e.g.* Rietveld refinement against powder diffraction intensities might be performed; the key differences here are that the structural models generally contain

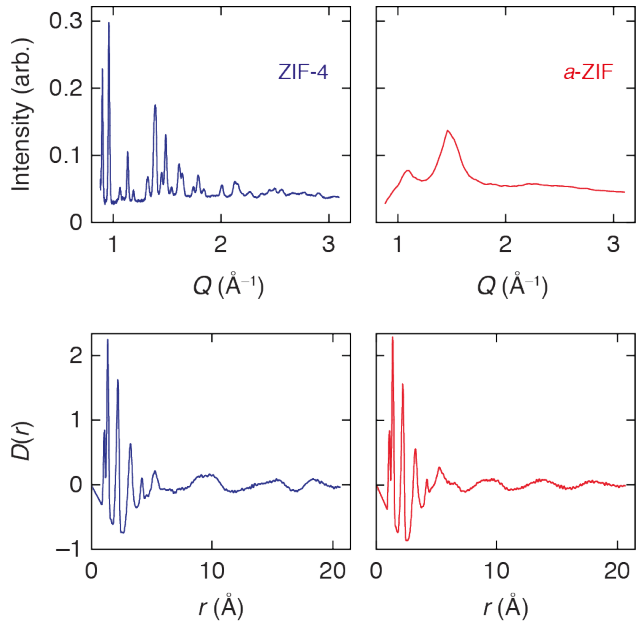

Fig. 3 The diffraction behaviour of topologically-disordered materials. The top panels show experimental neutron diffraction data collected for (left) the crystalline ZIF-4 polymorph and (right) the amorphous *a*-ZIF phase with identical composition. During TIA all of the sharp Bragg diffraction peaks observed for ZIF-4 (measured here as a function of scattering vector $Q = 4\pi \sin\theta/\lambda$) are successively replaced by broad diffuse scattering features that cannot be analysed using standard crystallographic approaches. The "peaks" in the *a*-ZIF diffraction pattern are not indexable in terms of a unit cell, but instead reflect the regions of maximum scattering intensity in the original ZIF-4 diffraction pattern. Fourier transform of the diffraction patterns gives the PDFs $D(r)$ shown in the lower panels, which represent the weighted probability of finding pairs of atoms separated by a given distance. The PDF is well-defined even in the absence of long-range periodicity. Here the two functions are essentially identical up to $r \simeq 6$ Å, indicating that the local ZIF coordination environment is preserved in the TIA phase. The resolution of the PDF depends on the maximum value of Q to which the diffraction pattern is reliably measured; these PDFs are obtained using $Q_{max} = 40$ Å^{-1}, which is substantially larger than the value $Q_{max} \simeq 6$ Å^{-1} achievable using standard laboratory X-ray diffractometers.

many thousands of atoms and so a non-deterministic fitting algorithm (*e.g.* Reverse Monte Carlo, or RMC; Ref. 15) is required in order to sample effectively the vast available configurational space. That analogous refinements for *a*-ZIF using starting models based on crystalline ZIF polymorphs do not provide convincing fits to data strongly suggests it is more correct to think of the structure of *a*-ZIF in terms of a CRN than in terms of a periodic network with a large-amplitude distortions of its constituent linkers.

A conceptually-similar model has recently been proposed to describe the structure of "PAF-1" (PAF = porous aromatic framework), a highly-stable organic network polymer which exhibits one of the most extreme accessible surface areas known (BET surface area 5640 m^2 g^{-1}; Langmuir surface area, 7100 m^2 g^{-1} by N_2 sorption).[11,16] As for the *a*-ZIF described above, the X-ray diffraction pattern of PAF-1 exhibits no Bragg component. Yet the broad features in this diffraction pattern, together with ^{1}H MAS NMR measurements and also the N_2 sorption isotherms can all be explained in terms of a structural model derived from the CRN of SiO_2 [Fig. 2(c)]. To the best of our knowledge, a PDF investigation has not been reported for this system; however, one might anticipate that such a study would be particularly useful in verifying whether the CRN model proposed in Ref. 11 is indeed valid. Most PAFs are amorphous, and in these systems the absence of long-range periodicity is attributed to the irreversibility of the coupling reaction used during polymerisation.[16] Interestingly, the bridging ligand length used in PAF synthesis appears to play a crucial role in determining microporosity: too small a linker and the network is too densely packed; too large a linker and the network either has sufficient flexibility to become interpenetrated or the system becomes mesoporous. So it is possible also to establish local-structure/property relationships even in these amorphous systems despite the inherent difficulty in determining their structures.

Both the families of *a*-ZIFs and of PAFs show considerable chemical and topological diversity, so there is genuine scope for meaningful materials optimisation in both cases. This allows, in principle at least, the development of new classes of amorphous materials in which in the various attractive mechanical and optical properties of amorphous solids are coupled with desirable chemical and physical functionalities accessible using molecular framework chemistry. So, for instance, the incorporation of chiral ligands, transition metals, or lanthanides provides strategies for developing, respectively, chiral, magnetic or luminescent glasses. Moreover, because macroscopic flow is observed during TIA of ZIFs,[10] there remains the possibility of machining (or casting) homogenous ZIF-based optical lenses [Fig. 4]. If one could find a method of retaining some intrinsic microporosity then such lenses could display guest-dependent focal lengths, or act as sensors for the presence of particular sorbates.

Finally, we note that the ability to 'switch' molecular frameworks between crystalline and amorphous states is strongly reminiscent of DVD-RAM technology, which is based on similar behaviour in the phase-change chalcogenides. In these systems the extent of crystallinity functions as a means of storing data: the different optical response of the two states allows data reading, and in the case of *a*-ZIFs localised heating might allow a mechanism for switching states (and hence data writing) [Fig. 5].[17] The possibility of irradiation-driven amorphisation/crystallisation in molecular frameworks would

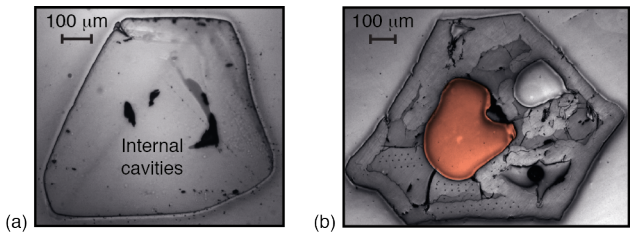

Fig. 4 Plastic flow during TIA in *a*-ZIF. Representative micrographs of *a*-ZIF monoliths obtained by heat-treatment of single crystals of ZIF-4: (a) before, and (b) during subsequent transformation to ZIF-zni.[10] A peculiar feature of both is the inclusion of curved cavity regions within the interior of the monoliths (one in (b) is highlighted in red), the presence of which is attributed to density collapse of the ZIF matrix during TIA. The edges of the monoliths—which originate as facets of the ZIF-4 crystals—can also be seen to assume curved morphologies. Both observations indicate macroscopic flow during TIA.

appear to be—at least at this stage—a largely unexplored area of research.

3 Static disorder

Whereas the amorphous molecular frameworks accessed through TIA or precipitation routes have network topologies that are distinct from those of their crystalline analogues, it is possible also to introduce sufficient disorder within crystalline molecular frameworks *without making or breaking bonds* that the systems come to appear just as disordered. Perhaps the most straightforward relevant mechanism is that of applying hydrostatic pressure. It has been known for some time that various oxide-based frameworks will exhibit pressure-induced amorphisation (PIA) at pressures of *ca* 10–100 GPa,[18] but the flexible bonding arrangements in molecular frameworks translate to much reduced critical pressures in the case of molecular frameworks. Examples include the canonical metal–organic framework MOF-5 (critical pressure, $p_c = 3.5$ MPa)[19] and also various ZIFs (p_c(ZIF-8) = 0.34 GPa; p_c(ZIF-4) = 6.5 GPa).[20,21] In each case there is a sizeable density increase during amorphisation that reflects structural collapse, and again the process is observable experimentally by monitoring the disappearance of Bragg intensities in diffraction patterns. But the fact that the MOF-5 amorphisation process is reversible on pressure release, and also that *a*-ZIF-8 retains some microporosity implies that the amorphous networks produced during this process carry some 'memory' of the original crystalline arrangement. As for the "topologically-ordered glass" phase of SiO_2 obtained by PIA of a siliceous zeolite,[22] the absence of periodicity in pressure-amorphised molecular frameworks reflects not a change in network connectivity but rather the existence of large incoherent static displacements of the molecular linkers [Fig. 6].

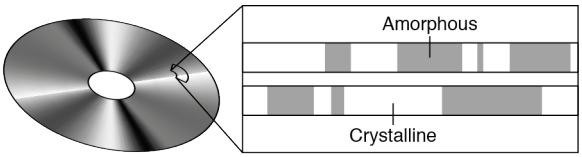

Fig. 5 At its simplest level, data storage in DVD-RAM media exploits both the different optical responses of amorphous and crystalline polymorphs (which enables data reading) and also the ability of materials such as AgInSbTe to switch between amorphous and crystalline states under laser irradiation.[17]

One important potential application of this PIA behaviour concerns the immobilisation of radioactive byproducts of nuclear energy production. The general strategy is straightforward: a crystalline precursor framework is loaded with radioactive guest (*e.g.* I_2) and subsequently exposed to hydrostatic pressures capable of initiating amorphisation

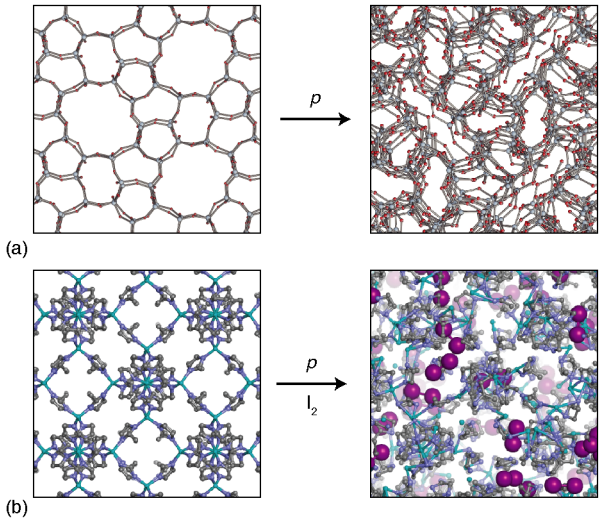

Fig. 6 Topologically-ordered amorphous phases. (a) The open network structure of a siliceous zeolite silicalite-1-F undergoes a massive volume collapse under application of hydrostatic pressures. The collapsed phase is amorphous in the sense that its diffraction pattern contains no sharp Bragg reflections, but its PDF can be interpreted in terms of a statically-disordered structure with the same network connectivity as the original crystalline phase but with large-amplitude uncorrelated displacements of large regions of the structure.[22] (b) A similar mechanism could also describe PIA in the molecular framework ZIF-8. Guest molecules (*e.g.* I_2, shown here as large purple spheres) included within the pore structure of the crystalline phase are effectively trapped within the amorphised host, despite the latter retaining its original network connectivity. Adapted with permission from *J. Am. Chem. Soc.*, 2009, **131**, 12333–12338. Copyright 2009 American Chemical Society.

[Fig. 6(b)].[23] The guest effectively becomes trapped during the framework collapse associated with PIA, with subsequent leaching reduced by at least an order of magnitude in the case of (*a*-)ZIF-8. Structural evidence for the retention of I_2 within the pore network of *a*-ZIF-8 was obtained using X-ray PDF measurements, illustrating how—despite the absence of long-range structural periodicity—it remains possible to structurally characterise host-guest interactions within an amorphous system.

The presence of guest molecules within the pore system of a molecular framework effectively places the network itself under negative (*i.e.* internal) hydrostatic pressure. Consequently the removal of guest molecules—for example by straightforward desoprtion—can have a similar effect on the framework as would application of positive (*i.e.* external) hydrostatic pressure. Just as PIA is found to occur in a number of different molecular frameworks, so too is it the case that desorption-induced amorphisation (DIA) is not uncommon. The mechanisms of the two effects also appear to be very similar in that the framework topology is preserved during DIA with crystallinity often recoverable *via* subsequent re-sorption. We illustrate this point with two examples: one recent and one historic.

The metal–organic framework Cu-SIP-3 is of current interest for its selective uptake and delivery of nitrous oxide for use in biomedical devices [Fig. 7(a)].[24–26] Its framework chemistry is characterised by the presence of some strong and some weak node–linker interactions, the latter having the effect of facilitating large-scale rearrangement of framework components through flexing of weak bonds. The as-prepared (hydrated) form of Cu-SIP-3 is obtainable as high-quality single crystals. Gentle dehydration over the temperature range $370 < T < 405$ K is accompanied by apparent loss of crystallinity, but single-crystallinity is restored by further annealing at temperatures above 405 K [Fig. 7(b)].[24] Not only are the network connectivites of the hydrated and dehydrated forms identical, but the orientation matrices determined during single crystal diffraction measurements indicate that the macroscopic orientation of the pre- and post-transition single crystals are one and the same [Fig. 7(c)]. Consequently the amorphous intermediate must retain a 'memory' of the network geometry and orientation; in particular it is certainly anisotropic. This transformation is all the more remarkable for the large structural reorganisations (several Å) and volume collapse ($> 20\%$) involved; moreover the process is entirely reversible on exposure to H_2O.

X-ray PDF measurements have played a crucial role in determining the mechanism for this transformation.[25] They suggest that the amorphous intermediate, which is partially hydrated, is not describable as a simple superposition of two end-member crystalline forms, but instead reflects the same sort of uncorrelated large-scale translations associated with PIA. On exposure to NO gas, the dehydrated phase appears once more to lose its crystallinity as the network re-opens to accommodate the NO guest (effectively the reverse process to that shown in Fig. 7). The maximum pressures of NO loading investigated (1 atm) were not sufficiently high to observe reformation of the fully-loaded crystalline phase, but the PDF measurements are consistent with analogous (re/de)-sorption mechanisms for H_2O and NO loading. So, in summary, the very structural flexibility that allows selective guest uptake in Cu-SIP-3 is the same motif responsible for the crystalline–amorphous transitions observed.

Our historic example concerns the homochiral 1,3,5-benzenetricarboxylate (*btc*) frameworks of general formula $Ni(btc)_{2/3}(py)_2Y\cdot\{guest\}$ (*py* = pyridine; Y = bis(alcohol) or diol) as described in Ref. 27. Depending on the nature of the alcohol ligand(s), this system crystallises as either a doubly- or a fourfold-interpenetrated (10,3)-a network. The use of 1,2-propanediol templates one of the former systems; ethanol templates one of the latter systems. So, starting with a crystalline sample of the porous, doubly-interpenetrated 1,2-propanediol framework, thermal desolvation then gives an X-ray amorphous solid. Crystallinity returns on re-exposure of this amorphous solid to 1,2-propanediol—an observation which in principle could be accounted for by a mechanism of dissolution and growth. Yet such a mechanism can in fact be discounted because exposure of the same desolvated amorphous phase to ethanol vapour initially yields a crystalline ethanol-containing phase which is doubly- rather than quadruply-interpenetrated. This metastable phase reorganises itself over time into the stable ethanolic configuration in which four (10,3)-a nets interpenetrate. Consequently the disordered desolvated intermediate must retain a memory of the original network topology of the 1,2-propanediol framework—and is consequently a rare (characterised) example of a doubly-interpenetrated amorphous solid.

In these two cases, the extent of static disorder is at its most extreme, in that there is complete loss of structural periodicity. A somewhat less extreme—but no less remarkable—type of static disorder is thought to be responsible for hysteretic sorption of CO_2 in the indium-carboxylate framework NOTT-202.[28] The material consists of two interpenetrating framework components: one is fully ordered, and the other is ordered over small length-scales but is only partially occupied throughout the entire solid [Fig. 8]. Consequently a sizeable portion of the solid is missing, with the defect sites surrounding these vacancies influencing the CO_2 sorption properties of the material. Indeed the unusual multistep adsorption profile observed experimentally can be mapped directly onto the concentrations of defects within this partially-occupied sublattice. It is argued that framework flexibility plays a crucial role in accommodating these defects and also allowing large gas uptake. We note that the general propensity for molecular framework

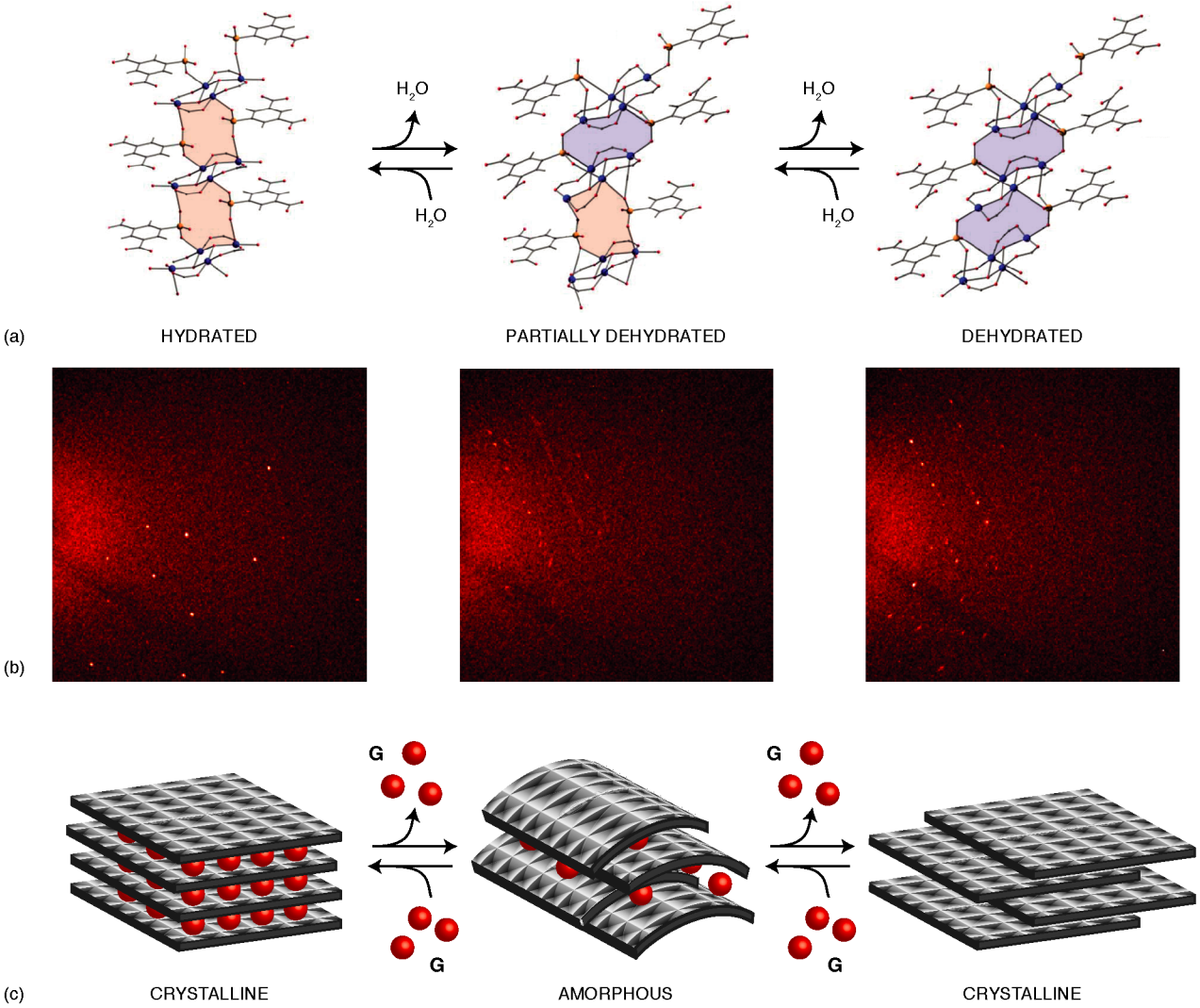

Fig. 7 Dehydration of crystalline Cu-SIP-3 proceeds via a poorly-ordered partially solvated intermediate, with single crystallinity recovered in the final anhydrous product.[24] (b) Single crystal diffraction patterns collected *in situ* during dehydration show the disappearance of strong Bragg reflections during intermediate stages. The mechanism proposed on the basis of X-ray PDF measurements[25] involves uncorrelated large-scale reorganisation of regions of the structure during dehydration as each successively becomes dehydrated. (c) A schematic representation of the process. Adapted with permission from Ref. 25 and *J. Am. Chem. Soc.*, 2010, **132**, 3605–3611. Copyright 2010 American Chemical Society.

materials of all types to exhibit large degrees of flexibility suggests that static disorder may in fact be more common in these materials than had previously been recognised.[29]

4 Dynamic disorder

For neutral molecular frameworks there is a direct correspondence between metal:ligand stoichiometries (determined by their respective charges) and the ratio of metal-to-ligand coordination numbers. But it is straightforward to engineer systems where these two factors do not correspond, such that anionic or cationic frameworks are formed instead, with charge balance achieved *via* inclusion of counterions within the framework pore system. A canonical example is given by the divalent transition metal formates: the metal-to-ligand charge ratio of (+)2:(−)1 is incompatible with the metal-to-ligand coordination preference ratio of 6:2. Consequently, transition metal formates favour the general formula $AM(HCOO)_3$ (A^+ = monocation) rather than $M(HCOO)_2$: in general they crystallise with a perovskite-like octahedral (cubic) net in order to

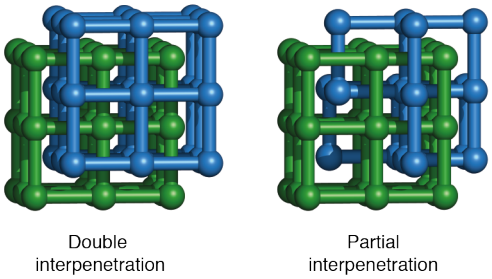

Fig. 8 Partial interpenetration provides defect sites for gas recognition and storage. The carboxylate-based framework NOTT-202 consists of one fully-occupied and one partially-occupied framework.[28] This is a very unusual form of interpenetration that suggests a new strategy for developing MOF-based catalysts: the fully-occupied framework provides mechanical stability, and the partially-occupied framework provides open binding sites for activation. By controlling vacancy correlations in may even prove possible to develop complex "active sites" within the pore-accessible volume. Adapted by permission from Macmillan Publishers Ltd: *Nature Materials*, Ref. 28, copyright 2012.

satisfy the coordination preferences of each component, but then must include extra-framework cations within the cubic pores of this net in order to obtain charge balance.

The relevance of a discussion concerning counterion inclusion in the broader context of structural disorder comes from the potential for symmetry-mismatch between the counterion and the shape of the framework cavity it occupies. In the case of many of the $AM(HCOO)_3$ formates, the room-temperature crystal structure has rhombohedral symmetry, with the A^+ ions occupying sites with point symmetry 32 (D_3).[30] Consequently if the counterion A^+ is chosen such that its molecular symmetry is distinct from D_3 (formally the condition we are considering is where the molecular point group of the counterion is not a supergroup of D_3) then there are only two possibilities: one is that the orientation of the counterion becomes disordered over multiple equivalent sites; the second is that the counterion adopts a single ordered orientation which then results in a symmetry-lowering distortion of the framework. The distinction between these two scenarios relies on the strength of cation–framework interaction energies relative to the available thermal energy k_BT, and consequently there is scope in all such systems for a temperature-driven order/disorder transition when these two energy scales coincide.

A pertinant example is that of the metal–organic framework $[(CH_3)_2NH_2]Mn(HCOO)_3$.[31] In this case, not only does the dimethylammonium (dma^+) counterion have lower symmetry (C_{2v}) than that of the D_3 crystallographic site it occupies, but it is also polar and so its orientational ordering can affect the macroscopic charge distribution within the the framework itself. Under ambient conditions, the dma^+ ions are *dynamically* disordered over three symmetry-related orientations; the framework exists in the non-polar space group $R\bar{3}m$. But when cooled below 190 K, the counterions no longer have sufficient thermal energy to sample all three orientations and instead settle into a single, ordered state [Fig. 9]. This molecular orientational ordering breaks the symmetry of the corresponding crystallographic site, causing a structural transition from $R\bar{3}m$ to the polar space group Cc. The crystallographic details here are important because they illustrate how structural disorder can affect a bulk material property—in this case, polarisation.

This order/disorder transition has a strong signature in the variable-temperature dielectric response of $[(CH_3)_2NH_2]Mn(HCOO)_3$.[31] Essentially what one is measuring in such an experiment is the extent to which charge can move within the framework in response to an applied electric field. In general, materials containing some dynamically-disordered dipolar component (*i.e.* a paraelectric material, by analogy with paramagnetism) exhibit a strong dielectric response because the dipoles simply rearrange in order to align with the applied field. Conversely, ordered phases exhibit a much weaker response because the dipoles are "trapped" in a single orientation. Certainly such a response is observed experimentally for this particular formate [Fig. 9], and this measurement provided strong additional support for the description of orientational ordering determined crystallographically.

An order/disorder transition is by no means unique to this particular formate: similar effects are observed when Zn^{2+} or

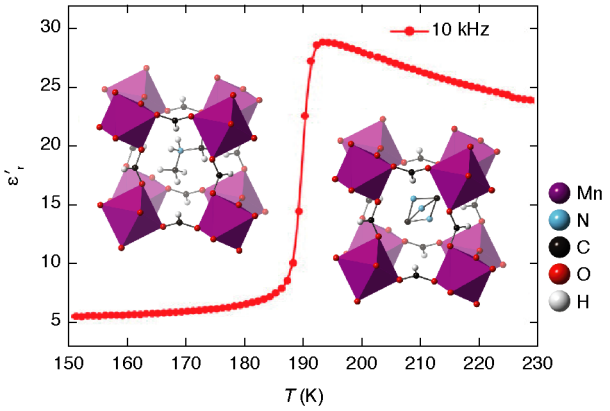

Fig. 9 A dynamic order/disorder transition in $[(CH_3)_2NH_2]Mn(HCOO)_3$. Dielectric measurements are particularly sensitive to such transitions: cation mobility in the high temperature (disordered) phase is reflected in a large dielectric response that is lost on cooling into the ordered phase. Here the order/disorder process involves reorientations of the dma^+ cation within the perovskite-like cubic pore. Adapted with permission from *Inorg. Chem.* 2010, **49**, 1510–1516. Copyright 2010 American Chemical Society.

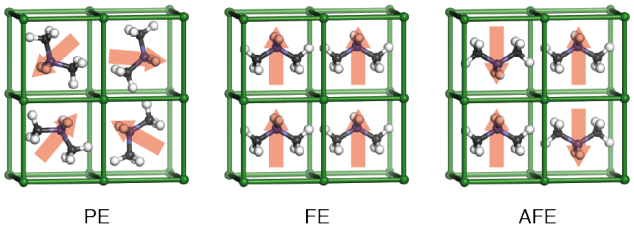

Fig. 10 Simple order and disorder scenarios in (anti)ferroelectric molecular frameworks. If an extra-framework counterion is polar then its orientation has the potential to influence the polarity of the crystal as a whole. Beyond some critical temperature, the available thermal energy is substantially larger than the counterion–framework interaction and the counterions may be considered to adopt a statistical distribution of possible orientations. In such a state, the molecular dipoles show no long-range order, and the phase is said to be paraelectric (PE). At low temperatures, there will not be sufficient thermal energy to overcome counterion–framework interactions and the system will order so as to optimise these interactions. This generally (but not always!) results in simple ordering of the molecular dipoles: if they are all aligned in the same sense then the phase is said to be ferroelectric (FE); if the alignment is antiparallel at nearest-neighbour distances then the phase is antiferroelectric (AFE). The FE phase is the only one with a net polarisation; this polarisation can be reversed by applying an external field—a process that lies at the heart of the many practical applications of ferroelectric materials.

Co^{2+} or Ni^{2+} replace Mn^{2+},[32,33] or when dma^+ is substituted by *e.g.* NH_4^+ (noting that T_d is not a supergroup of D_3).[34] Consequently, much of the focus within this very active field lies in understanding the dual roles of transition-metal and counterion substitution in determining (i) the ordering transition temperature, and (ii) the nature of the ordered phase—*i.e.* whether the local dipoles align in the same direction (ferroelectric ordering) or in opposite directions (antiferroelectric ordering) [Fig. 10]. Moreover, because magnetic ordering occurs for these same phases (albeit at substantially lower temperatures), there remains the exciting prospect of developing multiferroic frameworks where the order/disorder ferroelectric transition couples with magnetic ordering.[33,35]

The paradigm of symmetry-mismatch-driven dynamic disorder outlined here can also be seen to operate in what is chemically a very different molecular framework material: namely, imidazolium potassium hexacyanoferrate(III), $(H_2im)_2[KFe(CN)_6]$.[36] As for the formates, the anionic cyanide-bridged host framework of this material adopts a perovskite-like cubic topology, which at temperatures greater than 187 K also crystallises in the $R\bar{3}m$ space group. The approximately-pentagonal imidazolium cations (point group C_{2v}) are situated at the centres of the cubic pores (point symmetry D_3), and consequently are disordered over multiple orientations. In this case—and for reasons that are not well understood—there is actually a pair of dielectric anomalies at two distinct transition temperatures (158 and 187 K), with the lower-temperature phase transition corresponding to orientational ordering of the imidazolium ions and global symmetry lowering to the $C2/c$ space group. That there is such a strong correspondence between this system and the formates despite their different chemistries suggests the likely existence of many families of (anti-)ferroelectric molecular frameworks.

Our final example of a molecular framework that exhibits dynamic disorder concerns a system that is arguably of greatest interest for its unusual thermal expansion behaviour. Cadmium cyanide, $Cd(CN)_2$, consists of two interpenetrating diamond-like networks; this structure has cubic symmetry and so the thermal response of $Cd(CN)_2$ is inherently isotropic.[37] On heating, the unit cell volume of $Cd(CN)_2$ actually decreases; moreover this negative thermal expansion (NTE) effect is about 2–3 times stronger than the usual (positive) thermal expansion of conventional materials. Variable-temperature single crystal measurements of $Cd(CN)_2$ reveal two particularly anomalous effects, both of which indicate that dynamic disorder plays an important role in this system. First, the mean-squared displacement parameter of the Cd centre actually increases on cooling (ordinarily atoms should move less at lower temperatures);[37,38] and, second, the diffraction pattern contains an intense, highly-structured and temperature-dependent diffuse scattering component [Fig. 11(a)].[38]

The origin of these effects is a tendency at low temperatures for the Cd centres to occupy lower-symmetry sites of higher coordination number that are displaced away from the ideal tetrahedral site by *ca* 1 Å in each of six symmetry-related directions [Fig. 11(b)].[38] At temperatures below 150 K the Cd atoms do not have sufficient thermal energy to switch between sites and the framework symmetry is lowered accordingly. On heating beyond 150 K each Cd occupies all six sites in turn such that its average position is increasingly well described by the central position—the tetrahedral site. Because displacements away from this site require framework expansion (and hence displacements towards the central site allow compression), the dynamic disorder mechanism is coupled to the NTE effect.

The existence of structured diffuse scattering indicates that the displacement of one Cd centre is strongly correlated with that of its neighbours [Fig. 11].[38] Ordinarily, diffuse scattering is roughly three orders of magnitude weaker than Bragg scattering, but in this instance the diffuse component is particularly strong by virtue *both* of the large displacements *and* of the large X-ray scattering cross-section of the Cd atoms. In all likelihood, many—if not all—of the dynamically-disordered systems described above would exhibit structured diffuse scattering on some level because the orientation of any one extra-framework counterion is almost certainly not completely decoupled from that of its neighbours. While the interpretation

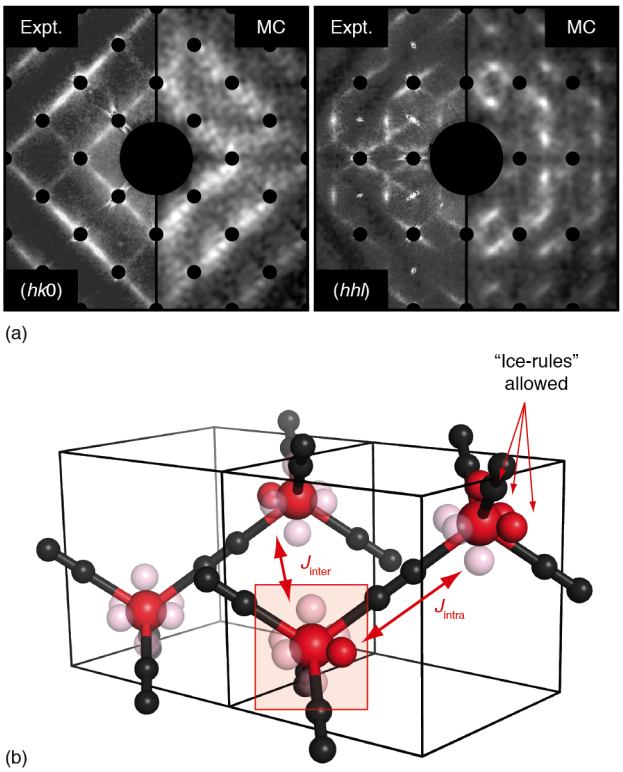

Fig. 11 Correlated disorder and structured diffuse scattering in $Cd(CN)_2$. (a; left-hand panels) Reconstructed $(hk0)$ and (hhl) cuts of reciprocal space for $Cd(CN)_2$ obtained using in-house single-crystal X-ray diffraction measurements. Bragg reflections have been obscured by black circles. (b) The disorder mechanism involves the displacement of Cd atoms from their average crystallographic position (large red spheres) by about 1 Å in one of the six symmetry-equivalent $\langle 100 \rangle$ directions (small red spheres). By taking into account the likely effect of one type of displacement on that of its neighbours (parameterised here by the coupling constants J_{inter} and J_{intra} for inter- and intra-framework correlations, respectively), it is possible to use Monte Carlo methods to calculate expected diffuse scattering patterns (a, right-hand panels).

of temperature-dependent diffuse scattering patterns is in general a nontrivial exercise,[39] the existence of such scattering is direct experimental evidence not only for dynamic disorder, but also for the importance of correlations in that disorder. Any inference concerning the interactions that control those local correlations can often be tested by using computational tools such as custom-made Monte Carlo simulations or software packages such as DISCUS to calculate the corresponding expected diffuse scattering patterns.[40] A qualitative match between calculated and observed diffuse scattering is usually taken as strong evidence to support the proposed local interaction model.

5 Reduced dimensionality

For the vast majority of the systems described in the various preceding sections, disorder arises by virtue of the low energy scale of key interactions in molecular frameworks—be those within the frameworks themselves or between the framework and some included component. Suitable choice of metal coordination preference and ligand connectivity can in fact yield materials where there are essentially no bonding interactions within certain directions. In this sense, columnar and layered systems—in which strong interactions are constrained to either one or two dimensions, respectively—essentially represent an extreme form of static disorder. Such systems can offer particularly attractive physical properties, including frustrated magnetism, intercalation chemistry, nanofabrication pathways and anomalous mechanical responses. For oxide-based frameworks, rational design of low-dimensional systems is often hampered by the propensity for oxide anions to interact either covalently or electrostatically with cations in all possible directions. Conversely, the specific binding preferences of particular molecular linkers can be exploited to impart strong directionality within molecular frameworks and hence enforce low dimensionality.

Here we focus initially on the family of pseudobinary transition-metal cyanides, chosen because the cyanide ion is an excellent example of a simple molecular linker with strongly directional bonding preferences.[43] In each of these compounds cyanide acts as a linear linker between metal centres, and hence the framework topology is really dictated by the coordination preference of the particular metal ion in question. For example, the group 11 monocations, which tend to favour linear coordination, form simple chain structures, whereas the group 10 dications, which exhibit the characteristic square-planar d^8 electronic configuration, form layered square grids instead [Fig. 12(a)].[42,44] In both cases the interchain/interlayer interactions are limited to dispersion forces and weak electrostatic interactions, and in nearly all cases these are not sufficiently strong to drive three-dimensional periodic ordering of the solid as a whole. Rather these materials exhibit strict crystalline periodicity only within the direction(s) which contain the strong metal–cyanide bonds and are disordered to various different extents in the perpendicular direction(s).[41] This situation parallels the existence of "stacking faults" in clay minerals (*e.g.* kaolinite[45]) and layered inorganic intercalation compounds (*e.g.* NbS_2; Ref. 46). In all cases, the absence of strong bonding interactions between layers gives rise to a lack of registration in the layer positions.

Were it possible to perform a single-crystal X-ray diffraction measurement for any one of these systems (noting that in most cases structural disorder prohibits growth of sufficiently-large crystals for such a measurement), then the reduced dimensionality of its structure would become apparent in the

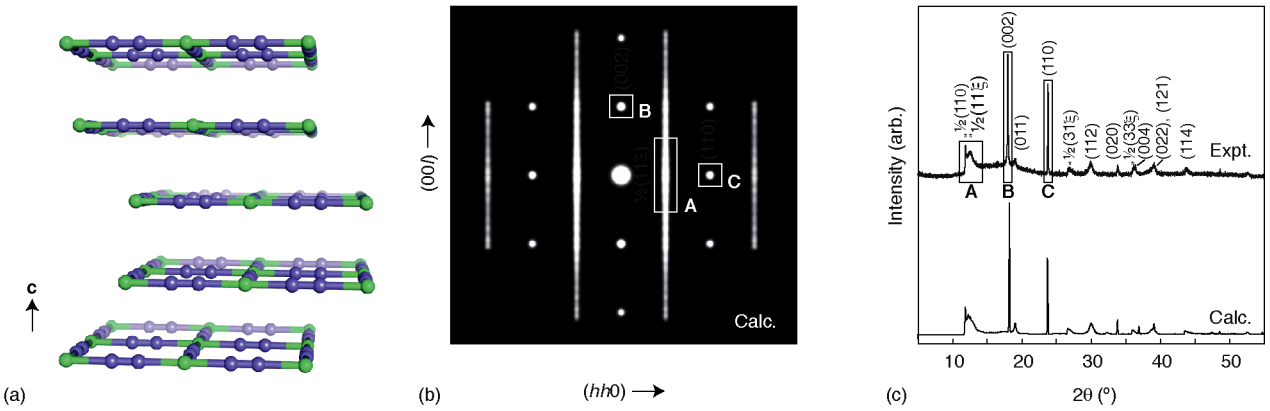

Fig. 12 Diffraction signatures of layered materials. (a) The structure of $Ni(CN)_2$ consists of square-grid layers that are well ordered in the layer directions, but have no periodic ordering in the perpendicular direction (labelled here as **c**).[41] (b) The hypothetical single-crystal diffraction pattern of this material contains rods of diffuse scattering parallel to $\mathbf{c}^*$ (which is itself parallel to **c**) and also a set of "normal" Bragg reflections. (c) Consequently the powder diffraction pattern, which represents an orientational average over the single-crystal pattern shown in (b), contains a set of sharp reflections and also a number of broad features with asymmetric Warren peak shapes.[41,42] The correspondence between scattering features in (b) and (c) is indicated by the panels labelled 'A', 'B', and 'C'.

atypical diffraction pattern observed. For example, the diffraction pattern of layered materials appears to consist of typical Bragg reflections when viewed along a direction perpendicular to the layers, but rotation of the crystal away from this direction would reveal these "spots" to be the cross section of diffuse rods that run parallel to that layer stacking axis [Fig. 12(b)]. The orientational averaging implicit in a powder diffraction measurement means that these diffuse rods appear similar to Bragg reflections but carry a so-called Warren peak shape, which has a very broad and asymmetric tail [Fig. 12(c)].[47] Columnar systems behave in a conceptually similar manner: their "single-crystal" diffraction patterns would consist of *planes* of scattering, which also appear as asymmetric and broad Bragg-like features in a powder diffraction pattern. Consequently the observation of Warren peak shapes in powder diffraction patterns for molecular frameworks is a useful means of diagnosing the existence of severe packing disorder—and hence low dimensionality—even if obtaining a complete description of that disorder is not universally feasible.

From a functional materials perspective, what advantageous physical properties might one expect to find in these low-dimensional systems? First, the dynamical properties of low-dimensional materials are dominated by the effects of that reduced dimensionality. Vibrational motion in layered materials consists primarily of "rippling" of the layers; the analogous modes in columnar structures are skipping-rope-type transverse displacements.[48] Both types of distortion are unusual in the sense that their thermal population results in a contraction of the material within the strongly-bonded directions. Accordingly $Ni(CN)_2$ shows area-NTE within the layer directions just as AuCN and AgCN show linear NTE along the chain axis.[42,44] The same qualitative effects are seen for that simplest of two-dimensional materials—namely, graphite—as indeed they are for more complex layered molecular framework materials such as Cu-SIP-3.[49] In fact features that resemble diffuse rods are almost discernible in the diffraction pattern the amorphous-like partially-hydrated phase of Cu-SIP-3 [Fig. 7(b)] which suggests 2D behaviour during desolvation. Second, the very weak interactions between neighbouring parts of the same material can facilitate the "top-down" synthesis of nanostructured phases: for example lithium 2,2-dimethylsuccinate is a layered material with weak dispersive interactions between layers and as a consequence its polycrystalline powders are readily converted into exfoliated nanosheets *via* sonication.[50] And, third, there is the propensity for guest intercalation between layers or chains. This type of behaviour has long been known to occur for $Ni(CN)_2$,[51] and can induce visible colour changes during the switching between disordered and fully crystalline states in response to guest binding.[42]

6 Future directions

Perhaps by virtue of the central role played by crystallographic techniques in driving forward the entire field of molecular framework chemistry, for many years the emphasis within the community has (rightly) focussed on understanding well-ordered systems. The increasingly widespread realisation that structural *dis*order can play a crucial role in imparting unusual and useful physical properties of these same materials, coupled with the rapid development of techniques such as PDF

that enable structural characterisation of disordered systems, may yet result in some shift in emphasis towards disordered framework materials as potential candidates for the next generation of functional framework materials. In this review we have covered but a handful of different types of disorder in molecular frameworks, focusing primarily on families where there exist a number of characterised systems so that comparison is possible. But there are numerous other types of disorder—many of which are emerging in individual systems for the first time— and rather than devoting entire sections to each case, we use some of these as springboards for discussion of possible future directions of research in the field as a whole.

The first challenge will be to expand the number of framework systems known to exhibit well-characterised structural disorder. To this end, one increasingly popular method for synthesising disordered frameworks is that of mechanical grinding.[52,53] It has been shown, for example, that amorphous ZIF samples prepared by TIA and by mechanical grinding are essentially indistinguishable except for their particle size (and hence surface area). The ease with which ball milling preparations can be undertaken suggests a straightforward strategy with which to explore amorphisation processes across a very large number of different systems. This allows one to ask which chemical and which topological features allow or discourage amorphisation—questions which are key to rational design strategies that employ disorder, and also crucial to our understanding of the amorphisation process itself. An important challenge in this emerging field will be to understand in which instances the disordered phases produced by mechanosynthesis are truly amorphous and in which instances any apparent loss of crystallinity reflects nothing more than particle size effects. Indeed the border-line between nanocrystalline and amorphous descriptions of disordered phases remains an area of fertile discussion in the broader field.[54]

As we have seen, disorder need not imply a complete absence of crystallinity—in this vein another interesting approach that has emerged very recently is that of designing functionalised disordered MOFs using metal–ligand–fragment coassembly.[55] Here the approach is to use a small fraction of "defect" non-bridging linker fragments, which are incorporated within the MOF and which can subsequently be functionalised without any reduction in accessible pore volume. Essentially the majority linker holds the framework together, and the minority component acts as the location where catalysis, gas binding and/or chemical modification can take place. Looking further ahead, correlations between defect locations might then affect co-operativity in binding, or in the case of catalysis the formation of complex multi-component "active sites" within the framework lattice.

It is quite possible that the cooperative phenomena arising from geometric frustration could also be exploited in molecular framework materials. There are hints that "spin-ice"-like states play a role in driving NTE in the $Cd(CN)_2$ framework discussed above,[38] but there is perhaps more general scope for designing frustrated systems by following the strategy outlined in a recent study of liquid-crystal phases.[56] Here the approach is to functionalise linkers with appendages that would protrude into the pore system of the framework and then interact—either favourably or unfavourably—with each other. Depending on the geometry of the lattice, these interactions may then be frustrated, giving rise to complex ordering patterns that affect the dynamics and mesoscale structure of the system as a whole. One could envisage exploiting further the porosity of molecular frameworks to design a system where guest occupancies switch the key interactions from being favourable to unfavourable (or *vice versa*) and hence producing a large series of bulk property changes in response to guest binding.

The potential for molecular frameworks to behave as configurational glasses has not escaped notice: indeed some of the formates described above show relaxation processes that are clearly characteristic of such states.[32] At the very simplest level, these systems may help shed light on the broader phenomenology of the glass transition itself by simply by expanding the range of systems in which glassy behaviour is observed. But there is perhaps an emerging sense in which molecular frameworks might provide a more general playground for the exploration of systems with anomalous configurational entropies, by virtue of the extraordinary control over coordination geometry and network topology that is possible in these systems.[57]

Finally, and looking to active areas of research in functional oxide frameworks for inspiration, one might expect charge and compositionally-disordered states to play an increasingly high-profile role in molecular framework science. Already there are promising signs that cyanide-based frameworks may find application in ion storage and conduction applications—although it is perhaps not yet clear that they will outperform their oxide cousins.[58] As a final example, relaxor behaviour in perovskites relies on an ability to support concerted displacements of large nanoregions within a framework lattice;[3] surely the intrinsic flexibility of molecular frameworks might facilitate polar nanodomain formation, even if local polarisation densities are intrinsically lower? And, because ferroelectricity and magnetism can readily coexist in molecular frameworks, might not one hope to design magnetic relaxors based on molecular framework chemistry? Perhaps the only certainty amongst these various questions is that our collective understanding and ability to exploit disorder in these systems is at an early stage of its genesis. Our hope in this review has been to outline some of the various forms this disorder can take, and how it might give rise to a range of interesting and useful materials properties.

Acknowledgements

The authors gratefully acknowledge valuable discussions with M. J. Cliffe (Oxford), and financial support from the EPSRC (Grant No. EP/G004528/2) and the ERC (Grant No. 279075).

References

1 T. Fennell, P. P. Deen, A. R. Wildes, K. Schamlzl, D. Prabhakaran, A. T. Boothroyd, R. J. Aldus, D. F. McMorrow and S. T. Bramwell, *Science*, 2009, **326**, 415–417.
2 E. Božin, C. D. Malliakas, P. Souvatzis, T. Proffen, N. A. Spaldin, M. G. Kanatzidis and S. J. L. Billinge, *Science*, 2010, **330**, 1660–663.
3 G. Xu, Z. Zhong, Y. Bing, Z.-G. Ye and G. Shirane, *Nature Mater.*, 2006, **5**, 134–140.
4 M. O'Keeffe, *Chem. Soc. Rev.*, 2009, **38**, 1215–1217.
5 A. L. Goodwin, *Phys. Rev. B*, 2006, **74**, 134302.
6 J. M. Ziman, *Models of disorder. The theoretical physics of homogeneously disordered systems*, Cambridge University Press, Cambridge, 1979.
7 O. Delgado-Friedrichs, M. O'Keeffe and O. M. Yaghi, *Phys. Chem. Chem. Phys.*, 2007, **9**, 1035–1043.
8 D. E. Polk and D. S. Boudreaux, *Phys. Rev. Lett.*, 1973, **31**, 92–95.
9 M. G. Tucker, D. A. Keen, M. T. Dove and K. Trachenko, *J. Phys.: Condens. Matter*, 2005, **17**, S67–S75.
10 T. D. Bennett, A. L. Goodwin, M. T. Dove, D. A. Keen, M. G. Tucker, E. R. Barney, A. K. Soper, E. G. Bithell, J.-C. Tan and A. K. Cheetham, *Phys. Rev. Lett.*, 2010, **104**, 115503.
11 A. Trewin and A. I. Cooper, *Angew. Chem. Int. Ed.*, 2010, **49**, 2–5.
12 C. A. Young and A. L. Goodwin, *J. Mater. Chem.*, 2011, **21**, 6464–6476.
13 K. S. Park, Z. Ni, A. P. Côté, J. Y. Choi, R. Huang, F. J. Uribe-Romo, H. K. Chae, M. O'Keeffe and O. M. Yaghi, *Proc. Natl. Acad. Sci., U.S.A.*, 2006, **103**, 10186–10191.
14 T. D. Bennett, D. A. Keen, J.-C. Tan, E. R. Barney, A. L. Goodwin and A. K. Cheetham, *Angew. Chem. Int. Ed.*, 2011, **50**, 3067–3071.
15 R. L. McGreevy and L. Pusztai, *Mol. Simul.*, 1988, **1**, 359–367.
16 T. Ben, H. Ren, S. Ma, D. Cao, J. Lan, X. Jing, W. Wang, J. Xu, F. Deng, J. M. Simmons, S. Qiu and G. Zhu, *Angew. Chem. Int. Ed.*, 2009, **48**, 9457–9460.
17 T. Matsunaga, J. Akola, S. Kohara, T. Honma, K. Kobayashi, E. Ikenaga, R. O. Jones, N. Yamada, M. Takata and R. Kojima, *Nature Mater.*, 2011, **10**, 129–134.
18 P. Richet and P. Gillet, *Eur. J. Miner.*, 1997, **9**, 907–933.
19 Y. H. Hu and L. Zhang, *Phys. Rev. B*, 2010, **81**, 174103.
20 K. W. Chapman, G. J. Halder and P. J. Chupas, *J. Am. Chem. Soc.*, 2009, **131**, 17546–17547.
21 T. D. Bennett, P. Simoncic, S. A. Moggach, F. Gozzo, P. Macchi, D. A. Keen, J.-C. Tan and A. K. Cheetham, *Chem. Commun.*, 2011, **47**, 7983–7985.
22 J. Haines, C. Levelut, A. Isambert, P. Hébert, S. Kohara, D. A. Keen, T. Hammouda and D. Andrault, *J. Am. Chem. Soc.*, 2009, **131**, 12333–12338.
23 K. W. Chapman, D. F. Sava, G. J. Halder, P. J. Chupas and T. M. Nenoff, *J. Am. Chem. Soc.*, 2011, **133**, 18583–18585.
24 P. K. Allan, B. Xiao, S. J. Teat, J. W. Knight and R. E. Morris, *J. Am. Chem. Soc.*, 2010, **132**, 3605–3611.
25 P. K. Allan, K. W. Chapman, P. J. Chupas, J. A. Hriljac, C. L. Renouf, T. C. A. Lucas and R. E. Morris, *Chem. Sci.*, 2012, **3**, 2259–2564.
26 B. Xiao, P. J. Byrne, P. S. Wheatley, D. S. Wragg, X. Zhao, A. J. Fletcher, K. M. Thomas, L. Peters, J. S. O. Evans, J. E. Warren, W. Zhou and R. E. Morris, *Nat. Chem.*, 2009, **1**, 289–294.
27 C. J. Kepert, T. J. Prior and M. J. Rosseinsky, *J. Am. Chem. Soc.*, 2000, **122**, 5158–5168.
28 S. Yang, X. Lin, W. Lewis, M. Suyetin, E. Bichoutskaia, J. E. Parker, C. C. Tang, D. R. Allan, P. J. Rizkallah, P. Hubberstey, N. R. Champness, K. M. Thomas, A. J. Blake and M. Schröder, *Nature Mater.*, 2012, **11**, 710–716.
29 I. E. Collings, M. G. Tucker, D. A. Keen and A. L. Goodwin, *Z. Krist.*, 2012, **227**, 313–320.
30 P. Jain, N. S. Dalal, B. H. Toby, H. W. Kroto and A. K. Cheetham, *J. Am. Chem. Soc.*, 2008, **130**, 10450–10451.
31 M. Sánchez-Andújar, S. Presedo, S. Yáñez-Vilar, S. Castro-Garciía, J. Shamir and M. A. Señarís-Rodríguez, *Inorg. Chem.*, 2010, **49**, 1510–1516.
32 T. Besara, P. Jain, N. S. Dalal, P. L. Kuhns, A. P. Reyes, H. W. Kroto and A. K. Cheetham, *Proc. Natl. Acad. Sci., U.S.A.*, 2011, **108**, 6828–6832.
33 P. Jain, V. Ramachandran, R. J. Clark, H. D. Zhou, B. H. Toby, N. S. Dalal, H. W. Kroto and A. K. Cheetham, *J. Am. Chem. Soc.*, 2009, **131**, 13625–13627.
34 G.-C. Xu, X.-M. Ma, L. Zhang, Z.-M. Wang and S. Gao, *J. Am. Chem. Soc.*, 2010, **132**, 9588–9590.
35 L. Cañadillas-Delgado, O. Fabelo, J. A. Rodríguez-Velamazán, M.-H. Lemée-Cailleau, S. A. Mason, E. Pardo, F. Lloret, J.-P. Zhao, X.-H. Bu, V. Simonet, C. V. Colin and J. Rodríguez-Carvajal, *J. Am. Chem. Soc.*, 2012, **134**, 19772–19781.
36 W. Zhang, Y. Cai, R.-G. Xiong, H. Yoshikawa and K. Awaga, *Angew. Chem. Int. Ed.*, 2010, **49**, 6608–6610.
37 A. L. Goodwin and C. J. Kepert, *Phys. Rev. B*, 2005, **71**, 140301.
38 V. E. Fairbank, A. L. Thompson, R. I. Cooper and A. L. Goodwin, *Phys. Rev. B*, 2012, **86**, 104113.
39 T. R. Welberry and B. D. Butler, *Chem. Rev.*, 1995, **95**, 2369–2403.
40 T. Proffen and R. B. Neder, *J. Appl. Cryst.*, 1997, **30**, 171–175.
41 A. L. Goodwin, M. T. Dove, A. M. Chippindale, S. J. Hibble, A. H. Pohl and A. C. Hannon, *Phys. Rev. B*, 2009, **80**, 054101.
42 S. J. Hibble, A. M. Chippindale, A. H. Pohl and A. C. Hannon, *Angew. Chem. Int. Ed.*, 2007, **46**, 7116–7118.
43 A. G. Sharpe, *The Chemistry of Cyano Complexes of the Transition Metals*, Academic Press, London, 1976.
44 S. J. Hibble, G. B. Wood, E. J. Bilbé, A. H. Pohl, M. G. Tucker, A. C. Hannon and A. M. Chippindale, *Z. Krist.*, 2010, **225**, 457–462.
45 A. Plançon, R. F. Giese, R. Snyder, V. A. Drits and A. S. Bookin, *Clays Clay Miner.*, 1989, **37**, 203–210.
46 H. Katze, *Z. Krist.*, 2002, **217**, 127–130.
47 B. E. Warren, *Phys. Rev.*, 1941, **59**, 693–698.
48 I. M. Lifshitz, *Zh. Eks. Teor. Fiz.*, 1952, **22**, 475–486.
49 M. J. Cliffe and A. L. Goodwin, *J. Appl. Cryst.*, 2012, **45**, 1321–1329.
50 P. J. Saines, J.-C. Tan, H. H.-M. Yeung, P. T. Barton and A. K. Cheetham, *Dalton Trans.*, 2012, **41**, 8585–8593.
51 F. Aragòn de la Cruz and S. Miguel Alonso, *Naturwissensch.*, 1975, **62**, 298.
52 T. D. Bennett, S. Cao, J.-C. Tan, D. A. Keen, E. G. Bithell, P. J. Beldon, T. Friscic and A. K. Cheetham, *J. Am. Chem. Soc.*, 2011, **133**, 14546–14549.
53 S. Cao, T. D. Bennett, D. A. Keen, A. L. Goodwin and A. K. Cheetham, *Chem. Commun.*, 2012, **48**, 7805–7807.
54 M. M. J. Treacy and K. B. Borisenko, *Science*, 2012, **335**, 950–953.
55 J. Park, Z. U. Wang, L.-B. Sun, Y.-P. Chen and H.-C. Zhou, *J. Am. Chem. Soc.*, 2012, **134**, 20110–20116.
56 X. Zeng, R. Kieffer, B. Glettner, C. Nürnberger, F. Liu, K. Pelz, M. Prehm, U. Baumeister, H. Hahn, H. Lang, G. A. Gehring, C. H. M. Weber, J. K. Hobbs, C. Tschierske and G. Ungar, *Science*, 2011, **331**, 1302–1306.
57 P. J. Camp, A. Fuertes and J. P. Attfield, *J. Am. Chem. Soc.*, 2012, **134**,

6762–6766.
58 C. D. Wessells, R. A. Huggins and Y. Cui, *Nature Commun.*, 2011, **2**, 550.

